TECHNISCHE MECHANIK, Band 23, Heft 2-4, (2003), 92– 102
Manuskripteingang: 28. April 2003

Elastic Stress Ratchetting and Corotational Stress Rates

A. Meyers, H. Xiao and O. Bruhns

In memory of Jürgen Olschewski

It is well accepted that stresses should return to their original state after a closed elastic strain cycle. Here, we consider originally unstressed elements undergoing such cycles. We presume isotropic materials and use Truesdell's hypoelastic law. Depending on the applied corotational stress rate, undesirable stress ratchetting is observed in case of two commonly used objective rates, namely the Zaremba-Jaumann and the Green/Naghdi rates. The strain cycle reaches its original stress-free state when the logarithmic rate is applied.

1 Introduction

The concept of objectivity is important in the description of large elastic and inelastic deformations. A big number – in fact an infinite number – of objective stress rates has been presented in the past. The question arises, if all of them are equally suitable in the description of large elastic deformations. In particular, if relevant material line rotations occur, unreasonable phenomena, like stress oscillation in simple shear, dissipation in elastic strain cycles etc., may occur. Such unreliable results may have considerably negative effects in the description of elasto-plastic deformations, too, since the elastic deformation part, though sometimes small in comparison to the plastic deformation part, can substantially influence the result of the total deformation.

Dienes (1979) revealed the occurrence of stress oscillations in large elastic simple shear. A similar observation had been made by Lehmann (1972) seven years earlier for simple shear of a rigid plastic body. It is widely accepted that this unreasonable phenomenon results from the selected stress rate in the deformation description. In the last decades a large variety of objective stress rates has been presented to avoid the simple shear oscillations, all of them generally leading to different results. The question arises if the concept of objectivity is sufficient to account for cited problems and if the one or other rate will show other unreliabilities in other deformation processes.

Xiao et al. (1997a) presented a hypo-elasticity model based on the logarithmic stress rate (Xiao et al., 1997b). It has been shown (Xiao et al., 1999) that this model is exactly integrable and, moreover, is derivable from an elastic potential, thus combining hyperelasticity and hypoelasticity. Also, this property is exclusively bound to the logarithmic rate. It was shown (Bruhns et al., 2001), that this model showed proper results in the case of simple shear.

The question remains about results in the case of more complex strain paths. Lin (2002) proposed to consider a four phases plain strain cycle: extension, shear, compression and back to starting unstrained state. He showed that for such a cycle some non-corotational stress rates, namely Truesdell and Oldroyd rates, lead to erroneous results: stresses have a much too high value and residual stresses remain at the end of the cycle. In the case of three corotational stress rates, namely the Zaremba-Jaumann rate (Zaremba, 1903; Jaumann, 1911), the polar or Green/Naghdi rate (Green and Naghdi, 1965; Green and McInnis, 1967; Dienes, 1979, 1987; Scheidler, 1994) and the logarithmic rate (Lehmann et al., 1991; Reinhardt and Dubey, 1995, 1996; Xiao et al., 1996, 1997b, 1998b), the stress development is very similar; however, only in case of the logarithmic rate all stresses return back to their initial zero state at the end of the cycle.

For a simple shear deformation mode progressing monotonically, use of Jaumann rate was known to result in aberrant oscillatory shear stress response. Nevertheless, use of Naghdi rate etc. was found to produce reasonable monotonic shear stress response. On the other hand, for a single cycle of deformation mode recovering the original shape only once – although the most recent study has reported residual stresses resulting from use of Naghdi rate and other rates– their magnitudes may be regarded to be acceptable for realistic deformations. Here a pertinent

question may be: Whenever a strain cycle constantly repeats itself, how will the residual stresses or errors change with the cycle number? Will their magnitudes remain within an acceptable range or, to the contrary, steadily accumulate themselves and become larger and larger?

Since strain cycles and cyclic loading may be frequently met in realistic engineering problems and since they may repeat themselves in a quite large number, it seems important to investigate the foregoing questions related to repeated strain cycles and cyclic loading. It is well known that cyclic loading are related to the so-called strain ratchetting phenomena for inelastic models. In contrast with this, we shall study stress responses of the most widely used hypoelastic model under constantly repeated strain cycles. Here the main ideas are as follows:

a) We consider smooth strain cycles instead of piecewise, i.e. non-smooth, cycles;

b) we do not restrict ourselves to a single cycle but treat constantly repeated cycles; and finally

c) we study how residual stresses or errors change with the cycle number.

Specifically, we shall propose two types of simple strain cycles characterized by a single parameter φ in a smooth and unified manner. We shall show that similar ratchetting phenomena emerge for residual stresses. In particular, we demonstrate that, with a strain cycle repeating itself constantly, the magnitude of the residual stresses or errors resulting from Naghdi rate etc. will no longer stay within the acceptable range for the first cycle, but accumulate themselves steadily and almost linearly. To the contrary, for the logarithmic rate, no residual stresses emerge after each cycle, and the foregoing phenomena for residual stress or error accumulation thus disappear. In the first section the constitutive relation, i.e. the hypoelastic relation is given. In the following section the single parameter cycles are developed. Then, the numerical results are found by numerical integration; they are compared for the three corotational rates cited above.

2 Basic Relations

Let $\boldsymbol{X}$ be the position of a material particle in the reference configuration and $\boldsymbol{x}$ the position in the current configuration. The deformation gradient $\boldsymbol{F}$ describes the motion of the body

$$\boldsymbol{F} = \frac{\partial \boldsymbol{x}}{\partial \boldsymbol{X}}, \qquad \det \boldsymbol{F} > 0. \tag{1}$$

The particle velocity $\boldsymbol{v}$ and the velocity gradient $\boldsymbol{L}$ are defined by

$$\boldsymbol{v} = \dot{\boldsymbol{x}}, \qquad \boldsymbol{L} = \frac{\partial \boldsymbol{v}}{\partial \boldsymbol{x}} = \dot{\boldsymbol{F}}\boldsymbol{F}^{-1}, \tag{2}$$

where a superposed dot denotes the material time derivative. The deformation gradient $\boldsymbol{F}$ can be uniquely decomposed in the positive definite and symmetric left stretch tensor $\boldsymbol{V}$, embedded in the actual configuration, and the rotation tensor $\boldsymbol{R}$

$$\boldsymbol{F} = \boldsymbol{V}\boldsymbol{R}, \qquad \boldsymbol{R}^{-1} = \boldsymbol{R}^{\mathrm{T}}. \tag{3}$$

The objective left Cauchy-Green tensor $\boldsymbol{B}$ is computed from $\boldsymbol{V}$ and may be represented through its m distinct eigenvalues b_i and its eigenprojections $\boldsymbol{B}_i$ as

$$\boldsymbol{B} = \boldsymbol{V}^2 = \boldsymbol{F}\boldsymbol{F}^{\mathrm{T}} = \sum_i^m b_i \boldsymbol{B}_i, \qquad \sum_i^m \boldsymbol{B}_i = \boldsymbol{I}. \tag{4}$$

Herein $\boldsymbol{I}$ is the second order identity tensor. The following relations hold

$$\sum_i^m \boldsymbol{B}_i = \boldsymbol{I}, \quad \boldsymbol{B}_i\boldsymbol{B}_k = \begin{cases} \boldsymbol{0}, & i \neq k, \\ \boldsymbol{B}_i, & i = k. \end{cases} \tag{5}$$

For given eigenvalues b_i the eigenprojections $\boldsymbol{B}_i$ can be found over Sylvester's formula

$$\boldsymbol{B}_i = \delta_{1m}\boldsymbol{I} + \prod_{k\neq i}^m \frac{\boldsymbol{B} - b_k\boldsymbol{I}}{b_i - b_k}, \tag{6}$$

where δ_{ik} is the Kronecker symbol. The velocity gradient is additively decomposed in the symmetric and objective deformation rate $\boldsymbol{D}$ and the skew-symmetric vorticity $\boldsymbol{W}$

$$\boldsymbol{L} = \boldsymbol{D} + \boldsymbol{W}\,, \qquad \boldsymbol{D} = \frac{1}{2}(\boldsymbol{L} + \boldsymbol{L}^{\mathrm{T}}) = \boldsymbol{D}^{\mathrm{T}}\,, \qquad \boldsymbol{W} = \frac{1}{2}(\boldsymbol{L} - \boldsymbol{L}^{\mathrm{T}}) = -\boldsymbol{W}^{\mathrm{T}}\,. \tag{7}$$

The corotational – not necessarily objective – rate of a symmetric time-dependent tensor $\boldsymbol{A}$ is defined by

$$\boldsymbol{A}^{\circ *} = \dot{\boldsymbol{A}} + \boldsymbol{A}\boldsymbol{\Omega}^{*} - \boldsymbol{\Omega}^{*}\boldsymbol{A}\,, \tag{8}$$

where $\boldsymbol{\Omega}^{*}$ is the skew-symmetric spin tensor. Xiao et al. (1998a) showed that the most general form of objective corotational rates is related to the spin

$$\boldsymbol{\Omega}^{*} = \boldsymbol{W} + \sum_{i\neq k}^{m} h\left(\frac{b_i}{I_1}, \frac{b_k}{I_1}\right) \boldsymbol{B}_i \boldsymbol{D} \boldsymbol{B}_k\,. \tag{9}$$

Herein, I_1 is the first basic invariant of $\boldsymbol{B}$ and the spin function h enjoys the property $h(x,y) = -h(y,x)$. Particularly, the spins related to three well known objective rates considered here are (Xiao et al., 1998a)

- for the Zaremba-Jaumann rate $(\cdots)^{\circ \mathrm{J}}$ (Zaremba, 1903; Jaumann, 1911)

$$\boldsymbol{\Omega}^{\mathrm{J}} = \boldsymbol{W}\,; \tag{10}$$

- for the polar or Green/Naghdi rate $(\cdots)^{\circ \mathrm{R}}$ (Green and Naghdi, 1965; Green and McInnis, 1967; Dienes, 1979, 1987; Scheidler, 1994)

$$\boldsymbol{\Omega}^{\mathrm{R}} = \dot{\boldsymbol{R}}\boldsymbol{R}^{\mathrm{T}} = \boldsymbol{W} + \sum_{i\neq k}^{m} \frac{b_k - b_i}{b_k + b_i} \boldsymbol{B}_i \boldsymbol{D} \boldsymbol{B}_k\,; \tag{11}$$

- for the logarithmic rate $(\cdots)^{\circ \mathrm{L}}$ (Lehmann et al., 1991; Reinhardt and Dubey, 1995, 1996; Xiao et al., 1998b, 1996, 1997b)

$$\boldsymbol{\Omega}^{\mathrm{L}} = \boldsymbol{W} + \sum_{i\neq k}^{m} \left(\frac{b_k + b_i}{b_k - b_i} - \frac{1}{\ln b_k - \ln b_i}\right) \boldsymbol{B}_i \boldsymbol{D} \boldsymbol{B}_k\,. \tag{12}$$

In the following we consider the hypoelastic constitutive relation proposed by Truesdell and Noll (1965)

$$\boldsymbol{D} = \mathbb{K} : \boldsymbol{\tau}^{\circ *}\,. \tag{13}$$

$\boldsymbol{\tau}$ is the Kirchhoff stress tensor which is related to the Cauchy or true stress $\boldsymbol{\sigma}$ by

$$\boldsymbol{\tau} = (\det \boldsymbol{F})\boldsymbol{\sigma}\,. \tag{14}$$

We assume an isotropic unstressed initial state. The 4th order compliance tensor $\mathbb{K}$ is given by

$$\mathbb{K} = \frac{1}{2G}\left(\mathbb{I} - \frac{\nu}{1+\nu}\boldsymbol{I}\otimes\boldsymbol{I}\right)\,, \tag{15}$$

where $\mathbb{I}$ is the 4th order identity tensor, G is the shear modulus, and ν is Poisson's ratio. Note, that $\mathbb{K}$ is a constant tensor, i.e. it doesn't change in time. This will be considerably useful in the single parameter cycles proposed below.

3 Proposed Single Parameter Cycles

Assume a cycle that is dependent on a single parameter φ. We characterize the partial derivative with respect to φ by a prime, i.e.

$$(\cdots)' = \frac{\partial(\cdots)}{\partial\varphi} \quad \rightarrow \quad \dot{(\cdots)} = (\cdots)'\dot{\varphi}\,. \tag{16}$$

We introduce barred quantities $\bar{\boldsymbol{D}}$, $\bar{\boldsymbol{W}}$, $\bar{\boldsymbol{\Omega}}^{*}$, only depending on φ, by

$$\boldsymbol{D} = \bar{\boldsymbol{D}}\dot{\varphi}\,, \quad \boldsymbol{W} = \bar{\boldsymbol{W}}\dot{\varphi}\,, \quad \boldsymbol{\Omega}^{*} = \bar{\boldsymbol{\Omega}}^{*}\dot{\varphi}\,. \tag{17}$$

Since $\mathbb{K}$ is considered to be constant, equation (13) takes the form

$$\bar{\boldsymbol{D}} = \mathbb{K} : \left(\boldsymbol{\tau}' + \boldsymbol{\tau}\bar{\boldsymbol{\Omega}}^* - \bar{\boldsymbol{\Omega}}^*\boldsymbol{\tau}\right) \tag{18}$$

which constitutes a set of ordinary differential equations in φ. They are integrated by standard numerical integration schemes.

Whenever the deformation gradient $\boldsymbol{F}$ is known, we may evaluate the Cauchy-Green tensor $\boldsymbol{B}$ by equation (4), it's eigenvalues b_i, it's eigenprojections by equation (6), the barred deformation rate and vorticity by equations (2), (7), (17), the Green/Naghdi and the logarithmic spins by equations (11), (12) and hence the differential equations (equation (18)) for the stress development in function of the single parameter characterizing the imposed strain path and for different considered objective corotational stress rates.

3.1 Single Parameter Cycle 1

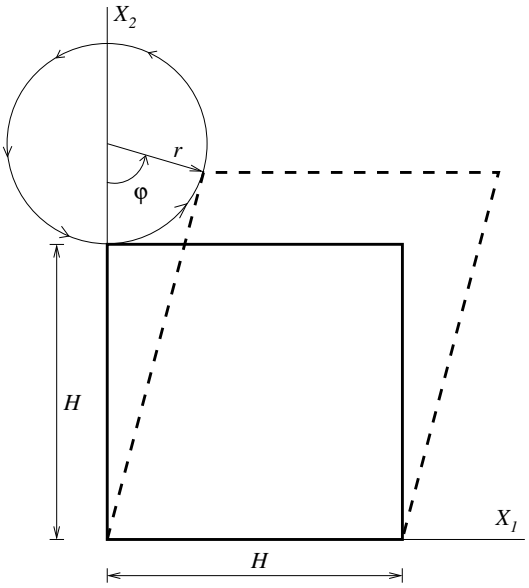

Figure 1: Cycle 1

Consider the square element of size $H \cdot H$ in Figure 1 which is embedded in the Cartesian reference system X_i. We impose a strain cycle where both upper corners rotate along a circle with radius r. Hereby the element is submitted to combined lengthening in X_2-direction and shear and remains a parallelogram in shape. We don't impose a deformation in direction X_3. The deformed element in the actual configuration is thus described by

$$\begin{aligned} x_1 &= X_1 + \frac{\sin\varphi \cdot r/H}{1 + (1-\cos\varphi)\cdot r/H} X_2 \\ x_2 &= (1 + (1-\cos\varphi)\cdot r/H) X_2 \\ x_3 &= X_3 \end{aligned} \tag{19}$$

¿From this and equation (1) we obtain the deformation gradient

$$\boldsymbol{F} = \begin{pmatrix} 1 & \dfrac{\sin\varphi \cdot r/H}{1 + (1-\cos\varphi)\cdot r/H} & 0 \\ 0 & 1 + (1-\cos\varphi)\cdot r/H & 0 \\ 0 & 0 & 1 \end{pmatrix} . \tag{20}$$

According to explanations given before, with equation (20) we may obtain the differential equation for the stress development and, hence, perform the numerical integration.

3.2 Single Parameter Cycle 2

Similarly to cycle 1, the square element of size $H \cdot H$ is submitted to a deformation of parallelogram shape (Figure 2), where the two upper corners now perform a circle of radius r to their right size. In difference to the deformation

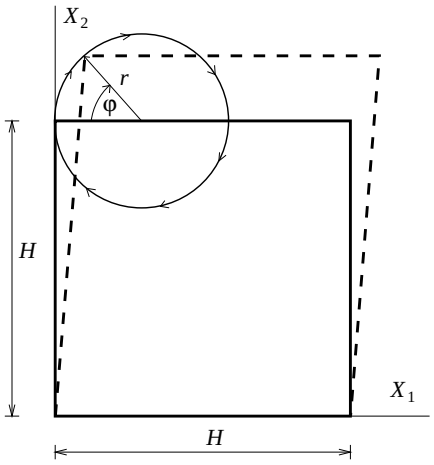

Figure 2: Cycle 2

in cycle 1, we have predominant element rotations involved in the deformation process. The deformed element is described in the actual configuration by

$$\begin{aligned} x_1 &= X_1 + \frac{(1-\cos\varphi)\cdot r/H}{1+\sin\varphi\cdot r/H} X_2 \\ x_2 &= (1+\sin\varphi\cdot r/H) X_2 \\ x_3 &= X_3\,, \end{aligned} \tag{21}$$

wherefrom

$$\boldsymbol{F} = \begin{pmatrix} 1 & \dfrac{(1-\cos\varphi)\cdot r/H}{1+\sin\varphi\cdot r/H} & 0 \\ 0 & 1+\sin\varphi\cdot r/H & 0 \\ 0 & 0 & 1 \end{pmatrix}. \tag{22}$$

4 Numerical Results

4.1 Cycle 1

For matter of example we select the ratio r/H to be 0.5, i.e. we consider relatively large elastic deformations.

In Figure 3 the normal Kirchhoff stresses τ_{11} and τ_{22} are plotted for the different corotational rates. It is seen that there are only marginal differences between the plots. The normal stress τ_{33} is almost equivalent to τ_{11} and, therefore, is not included in the graph. Since τ_{33} results from the same uncoupled differential equation for all considered rates, the plots would be exactly congruent.

Differences, however, are seen in the shear stress plot, Figure 4. At the end of the single cycle residual shear stresses are detected in case of Green/Naghdi and Jaumann rates.

In Figure 5, the development of Kirchhoff stresses is plotted for the case of the logarithmic rate and for 10 cycles. It is seen that the normal stresses are predominant. As expected, all stresses show an oscillatory behaviour.

For the same value of r/H the stresses in case of Green/Naghdi rate are plotted in Figure 6. We may observe the drift development of shear stress τ_{12} over the cycles, i.e. a stress ratchetting occurs. Also, the normal stresses τ_{11} (dotted line) and τ_{33} (dashed line), initially almost identical, start to deviate from each other. In case of Zaremba-Jaumann rate (Figure 7), apart of τ_{33}, which results from an uncoupled differential equation, all stresses start to show a drift. In case of the shear stress, this drift seems to be oscillatory. At the end of 10 cycles we identify undesirable residual stresses of remarkable magnitude.

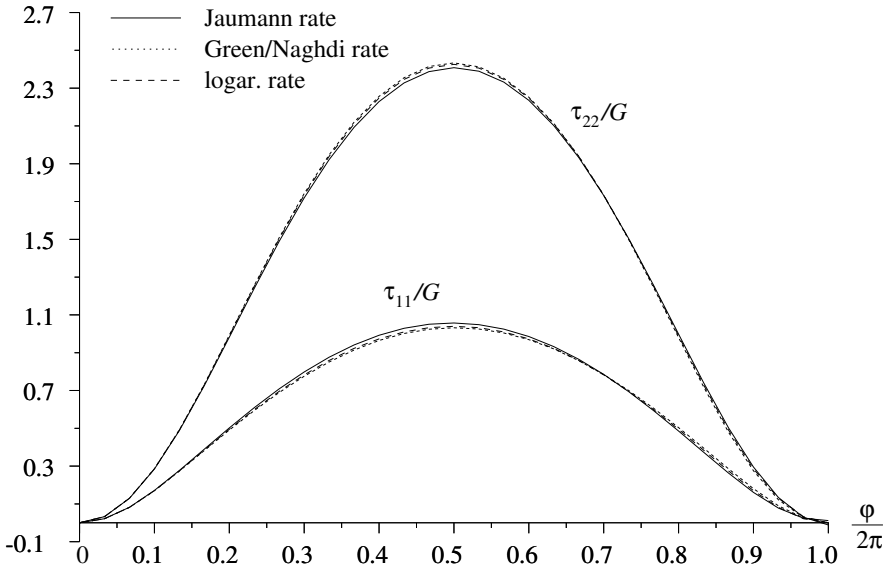

Figure 3: Normal stresses τ_{11} and τ_{22} in single cycle 1

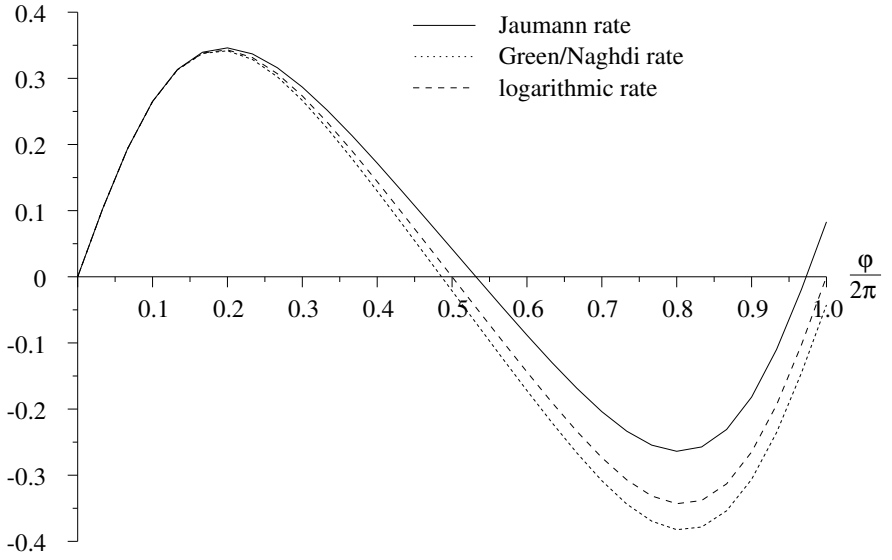

Figure 4: Shear stress τ_{12} in single cycle 1

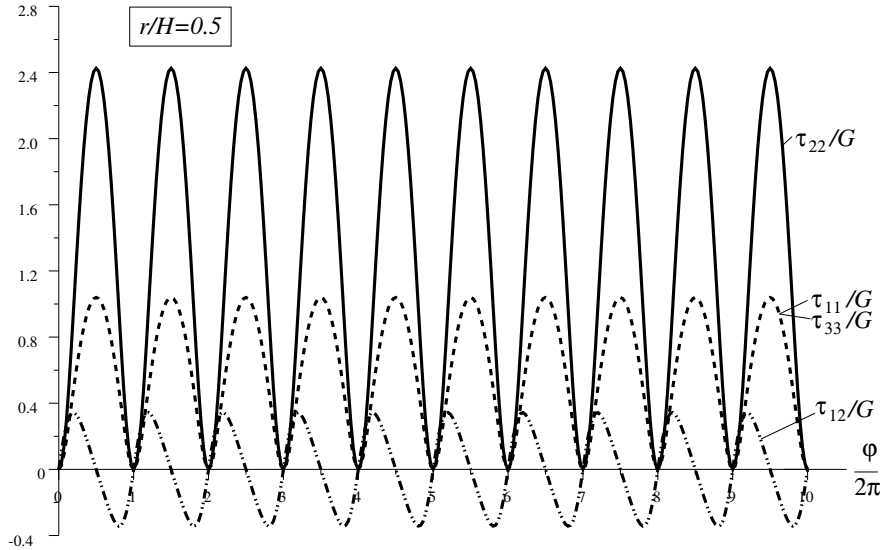

Figure 5: Cycle 1: Logarithmic rate

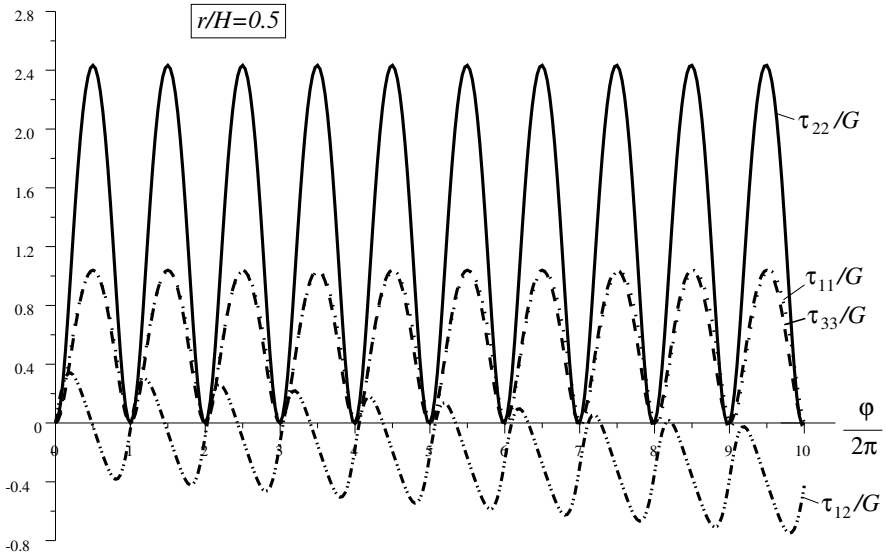

Figure 6: Cycle 1: Green/Naghdi rate

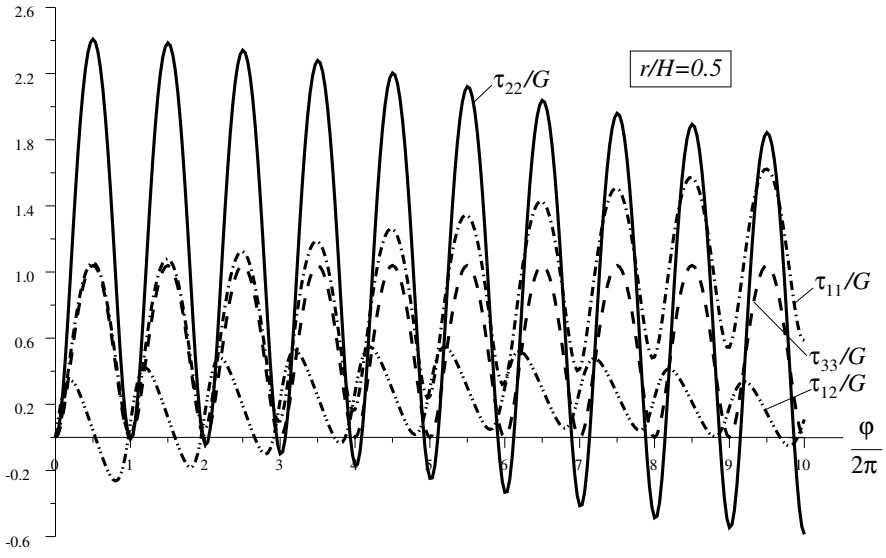

Figure 7: Cycle 1: Zaremba-Jaumann rate

4.2 Cycle 2

Cycle 2 accentuates material line rotations, i.e. the spin in the corotational derivative.

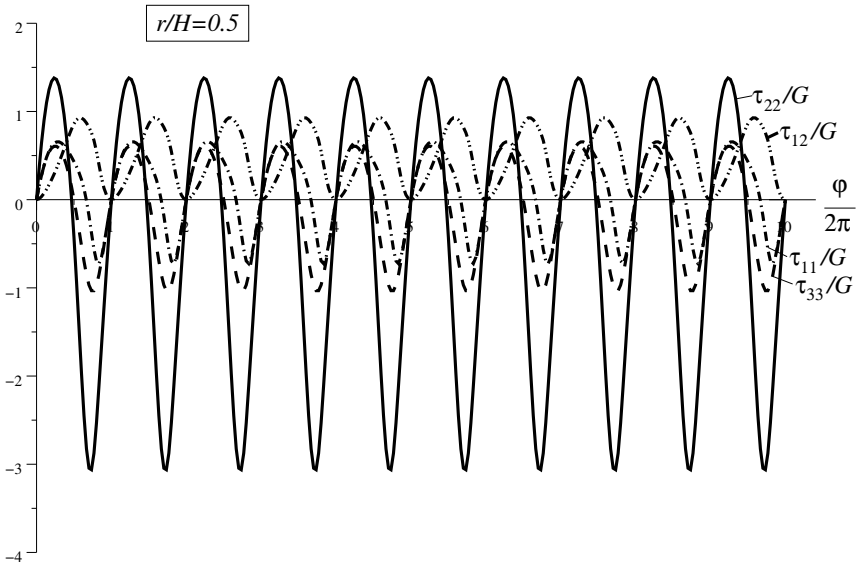

Figure 8: Cycle 2: Logarithmic rate

In Figure 8 the non-vanishing stresses are plotted in case of the logarithmic stress rate and in Figure 9 in case of

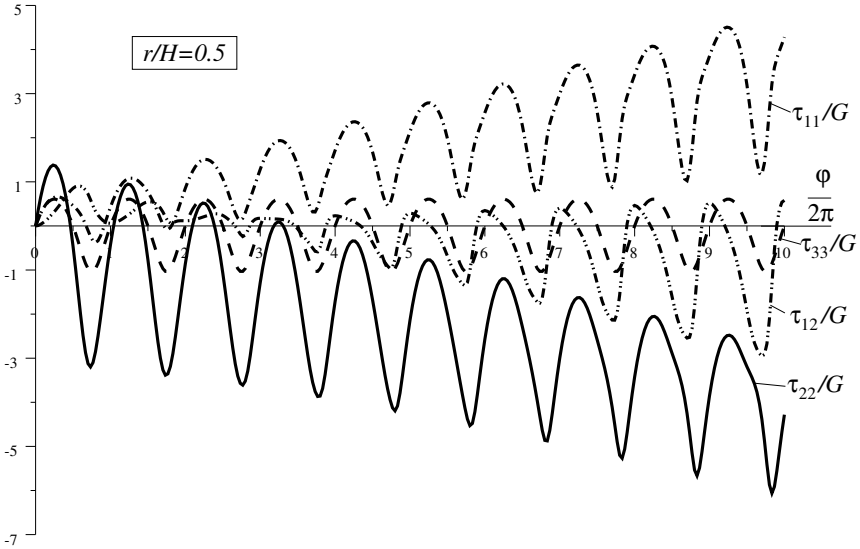

Figure 9: Cycle 2: Green/Naghdi rate

the Green/Naghdi rate. It may be seen that in the second case the normal stress τ_{11} fails to return to zero already after the first cycle. Apart of τ_{33}, of which the differential equation remains uncoupled, all stresses start to drift away and, moreover, to change their size. The resulting Kirchhoff stresses in case of Zaremba-Jaumann rate show hazardous behaviour after a few cycles. Stress drifts seem to be oscillatory. Especially in case of the shear stress τ_{12} results seem to be unpredictable.

4.3 Cycle 2: Stress Ratchetting and Error Accumulation

In the above examples the ratio r/H was chosen to be 0.5. This corresponds to relatively large strains. We now consider the much smaller ratio of 0.01. Elastic strains of this amount may occur for a variety of modern materials, e.g. composites, memory alloys, ceramics etc. Also for standard elastoplastic materials in nonlinear iterations the elastic predictor step can be related to strains of this amount.

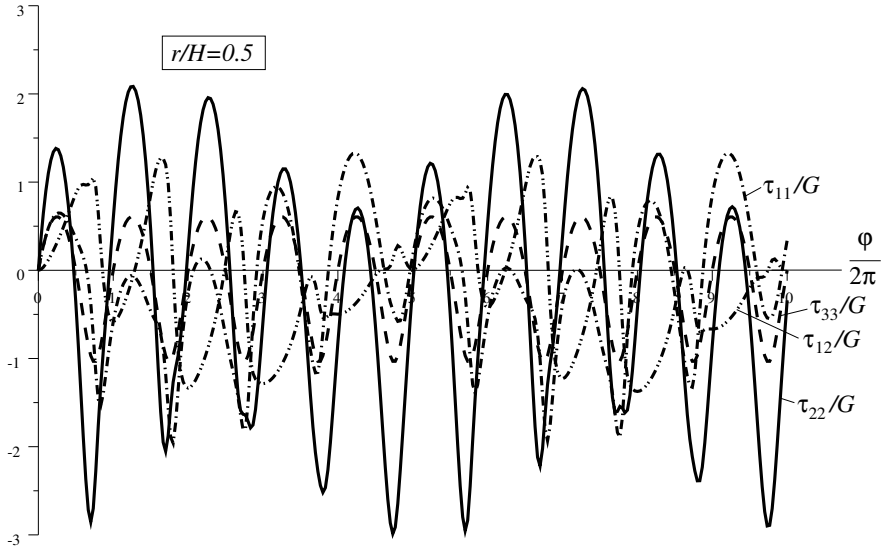

Figure 10: Cycle 2: Zaremba-Jaumann rate

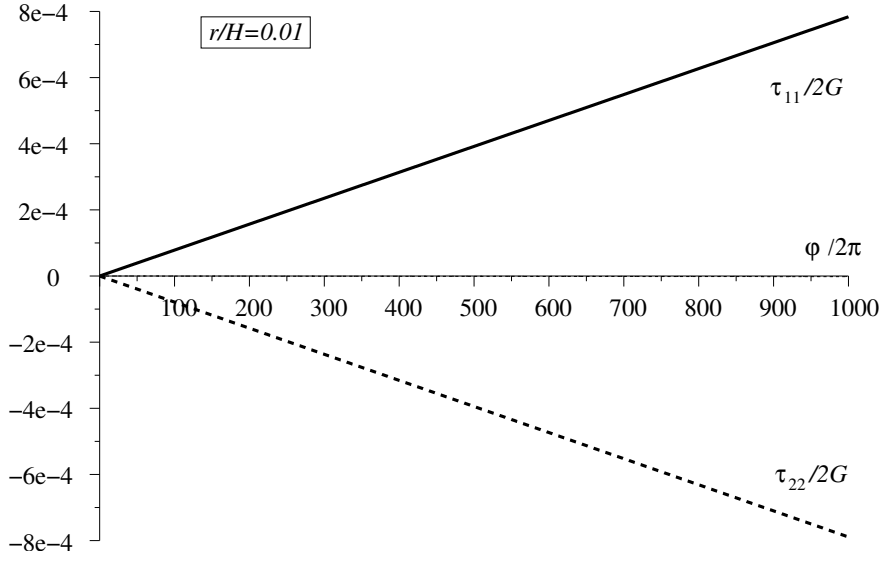

Figure 11: Cycle 2: Error accumulation, Green/Naghdi rate

In Figure 11 the error, i.e. the residual stress at the end of the cycle is plotted versus the number of cycles, for the case of Green/Naghdi rate. The residual stresses τ_{11} and τ_{22} are almost linearly increasing with the number of cy-

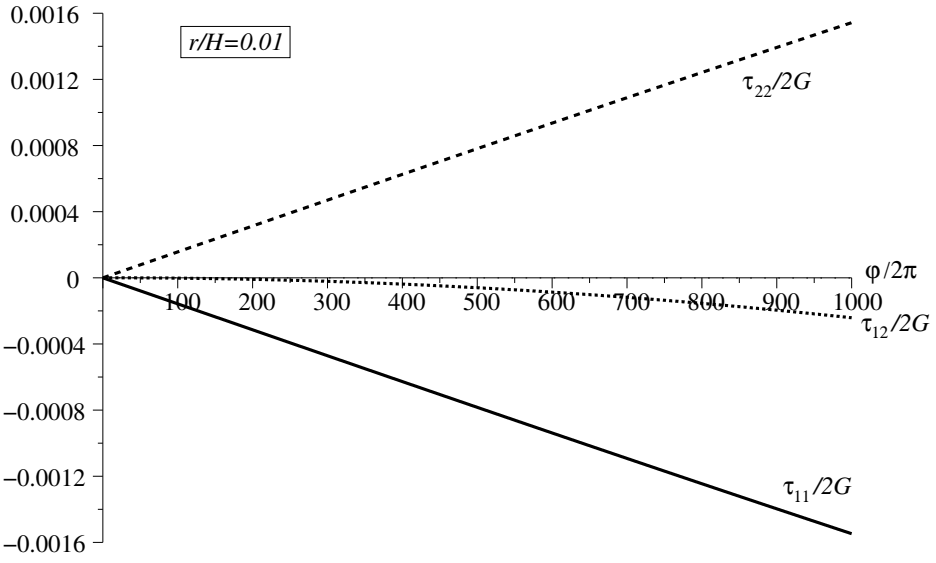

Figure 12: Cycle 2: Error accumulation, Zaremba-Jaumann rate

cles. The elastic limit, generally a few per mill of $2G$, can be reached or exceeded in course of the deformation. The situation appears to be still worse in case of the Zaremba-Jaumann rate (Figure 12). Not only the residual stresses raise to approximately double amount compared to the residual stresses in Green/Naghdi case, but additionally the shear stress τ_{12} starts to drift away. Such a drift is also observed in the Green/Naghdi rate case; however, the drift is negligibly small. It should be noticed that there are no residual stresses in case of the logarithmic rate, i.e. there is no error accumulation over the cycles.

5 Conclusion

For the simple Eulerian constitutive model, i.e. the hypoelastic equation of grade zero, three objective stress rates, namely the Green/Naghdi rate, the Zaremba-Jaumann rate and the logarithmic rate, have been compared in single parameter elastic cycles. It is shown that there are residual stresses at the end of the cycle for two of the three considered rates, i.e. stress ratchetting is observed. Only for the logarithmic rate stresses are returning to the vanishing, initial state at the beginning of the cycle, thus confirming the results found in Xiao et al. (1999).

References

Bruhns, O. T.; Xiao, H.; Meyers, A.: Large simple shear and torsion problems in kinematic hardening elasto-plasticity with logarithmic rate. *Int. J. Solids Struct.*, 38, (2001), 8701–8722.

Dienes, J. K.: On the analysis of rotation and stress rate in deforming bodies. *Acta Mechanica*, 32, (1979), 217–232.

Dienes, J. K.: A discussion of material rotation and stress rate. *Acta Mechanica*, 65, (1987), 1–11.

Green, A. E.; McInnis, B. C.: Generalized hypoelasticity. *Proc. Roy. Soc. Edinburgh*, A57, (1967), 220–230.

Green, A. E.; Naghdi, P. M.: A general theory of an elasto-plastic continuum. *Arch. Rat. Mech. Anal.*, 18, (1965), 251–281.

Jaumann, G.: Geschlossenes System physikalischer und chemischer Differentialgesetze. *Akad. Wiss. Wien, Sitzber. IIa*, pages 385–530.

Lehmann, T.: Anisotrope plastische Formänderungen. *Rom. J. Tech. Sci. Appl. Mech.*, 17, (1972), 1077–1086.

Lehmann, T.; Guo, Z. H.; Liang, H. Y.: The conjugacy between Cauchy stress and logarithm of the left stretch tensor. *Eur. J. Mech. A/Solids*, 10, (1991), 395–404.

Lin, R.: *Viscoelastic and Elastic-viscoelastic-elastoplastic Constitutive Characterizations of Polymers at Finite Strains: Theoterical and Numerical Aspects*. Ph.D. thesis, Bundeswehr University, Hamburg (2002).

Reinhardt, W. D.; Dubey, R. N.: Eulerian strain-rate as a rate of logarithmic strain. *Mech. Res. Comm.*, 22, (1995), 165–170.

Reinhardt, W. D.; Dubey, R. N.: Coordinate-independent representations of spins in continuum mechanics. *J. Elasticity*, 42, (1996), 133–144.

Scheidler, M.: The tensor equation $\boldsymbol{A}\boldsymbol{X} + \boldsymbol{X}\boldsymbol{A} = \boldsymbol{\Phi}(\boldsymbol{A}, \boldsymbol{H})$, with applications to kinematics of continua. *J. Elasticity*, 36, (1994), 117–153.

Truesdell, C.; Noll, W.: The non-linear field theories of mechanics. in: Handbuch der Physik. In: S. Flügge, ed., *Handbuch der Physik*, vol. III/3, Springer, Berlin (1965).

Xiao, H.; Bruhns, O. T.; Meyers, A.: A new aspect in kinematics of large deformations. In: N. K. Gupta, ed., *Plasticity and Impact Mechanics*, pages 100–109, New Age Intern. Publ. Ltd., New Delhi (1996).

Xiao, H.; Bruhns, O. T.; Meyers, A.: Hypo-elasticity model based upon the logarithmic stress rate. *J. Elasticity*, 47, (1997a), 51–68.

Xiao, H.; Bruhns, O. T.; Meyers, A.: Logarithmic strain, logarithmic spin and logarithmic rate. *Acta Mechanica*, 124, (1997b), 89–105.

Xiao, H.; Bruhns, O. T.; Meyers, A.: On objective corotational rates and their defining spin tensors. *Int. J. Solids Struct.*, 35, (1998a), 4001–4014.

Xiao, H.; Bruhns, O. T.; Meyers, A.: Strain rates and material spins. *J. Elasticity*, 52, (1998b), 1–41.

Xiao, H.; Bruhns, O. T.; Meyers, A.: Existence and uniqueness of the integrable-exactly hypoelastic equation $\boldsymbol{\tau}^{\circ *} = \lambda(\mathrm{tr}\boldsymbol{D})\boldsymbol{I} + 2\mu\boldsymbol{D}$ and its significance to finite inelasticity. *Acta Mechanica*, 138, (1999), 31–50.

Zaremba, S.: Sur une forme perfectionée de la théorie de la relaxation. *Bull. Intern. Acad. Sci. Cracovie*, (1903), 594–614.

Address: Dr.-Ing. Albert Meyers, Dr. Heng Xiao and Prof. Dr.-Ing. Otto Bruhns, Ruhr-University Bochum, D-44780 Bochum, Germany.
email: bruhns@tm.bi.rub.de.